

# Quantum Spin Hall Effect in Inverted Type II Semiconductors

Chaoxing Liu<sup>1,2</sup>, Taylor L. Hughes<sup>2</sup>, Xiao-Liang Qi<sup>2</sup>, Kang Wang<sup>3</sup> and Shou-Cheng Zhang<sup>2</sup>

<sup>1</sup> Center for Advanced Study, Tsinghua University, Beijing, 100084, China

<sup>2</sup> Department of Physics, McCullough Building, Stanford University, Stanford, CA 94305-4045 and

<sup>3</sup> Department of Electrical Engineering, UCLA, Los Angeles, CA 90095-1594

The quantum spin Hall (QSH) state is a topologically non-trivial state of quantum matter which preserves time-reversal symmetry; it has an energy gap in the bulk, but topologically robust gapless states at the edge. Recently, this novel effect has been predicted and observed in HgTe quantum wells[1, 2]. In this work we predict a similar effect arising in Type-II semiconductor quantum wells made from InAs/GaSb/AlSb. Because of a rare band alignment the quantum well band structure exhibits an “inverted” phase similar to CdTe/HgTe quantum wells, which is a QSH state when the Fermi level lies inside the gap. Due to the asymmetric structure of this quantum well, the effects of inversion symmetry breaking and inter-layer charge transfer are essential. By standard self-consistent calculations, we show that the QSH state persists when these corrections are included, and a quantum phase transition between the normal insulator and the QSH phase can be electrically tuned by the gate voltage.

PACS numbers:

Recently, a striking prediction of a quantum spin Hall (QSH) insulator phase in HgTe/CdTe quantum wells[1] was confirmed in transport experiments[2]. The QSH insulator phase is a topologically non-trivial state of matter reminiscent of the integer quantum Hall effect, but where time-reversal symmetry is preserved instead of being broken by the large magnetic field. The state is characterized by a bulk charge-excitation gap and topologically protected helical edge states, where states of opposite spin counter-propagate on each edge[3, 4, 5]. Unfortunately, high-quality HgTe/CdTe quantum wells are very special, and only a few academic research groups have the precise material control needed to carry out such delicate experiments. We are therefore lead to search for other, more conventional, materials that exhibit the QSH effect.

In this work we introduce a new material with the QSH phase, the InAs/GaSb/AlSb Type-II semiconductor quantum well in the inverted regime[6, 7, 8, 9, 10, 11]. We will show that this quantum well exhibits a subband inversion transition as a function of layer thickness, similar to the HgTe/CdTe system, and can be characterized by an effective four-band model near the transition. This model is similar to the model for HgTe/CdTe[1], but contains terms describing the strong bulk inversion asymmetry (BIA) and structural inversion asymmetry (SIA). In fact, due to the unique band alignment of InAs/GaSb/AlSb, the electron subband and the hole subband are localized in *different* quantum well layers. Additionally, the band alignment forces one to consider self-consistent corrections[12, 13, 14] which we will discuss below. Our results show that the asymmetric quantum well, with strong built-in electric field, can be electrically tuned through the phase transition using front and back gates. While this is of significant fundamental interest, it also allows one to construct a quantum spin Hall field effect transistor (FET) that exhibits an insulating “OFF” state with no leakage current, and a nearly dissipationless “ON” state with non-zero conductance via the topologi-

cal edge states.

The quantum well structures in which we are interested are asymmetric with AlSb/InAs/GaSb/AlSb layers grown as shown in Fig. 1. This is an unusual quantum well system due to the alignment of the conduction and valence band edges of InAs and GaSb. The valence band edge of GaSb is 0.15 eV *higher* than the conduction band edge of the InAs layer. The AlSb layers serve as confining outer barriers. The “conduction” subbands are localized in the InAs layer while the “valence” subbands are localized in the GaSb layer as illustrated in Fig. 1 (a). In this work we will focus on the regime where the lowest electron and hole subbands  $E_1, H_1$ , which are derived from the *s*-like conduction and *p*-like heavy-hole bands respectively, are nearly degenerate, and all other subbands are well-separated in energy. When the quantum well thickness is increased the energy of the  $E_1$  ( $H_1$ ) band edge is decreasing (increasing). At some critical thickness a level crossing occurs between  $E_1$  and  $H_1$ , after which the band edge of  $E_1$  sinks below that of  $H_1$ , putting the system into the inverted regime of Type-II quantum wells. Since the  $H_1$  band disperses downwards and the  $E_1$  band disperses upwards, the inversion of the band sequence leads to a crossing of the two bands, see Fig. 1 (b). Historically, the inverted regime of InAs/GaSb/AlSb quantum wells was described as a semi-metal without a gap[6]. However, Ref. [7] first pointed out that due to the mixing between  $E_1$  and  $H_1$ , a small gap ( $E_g$  in Fig 1 (b)) is generally opened, leading to bulk insulating behavior. This hybridization gap was later demonstrated in experiments[8, 9]. Therefore, just like in the HgTe/CdTe quantum wells, the inverted regime of InAs/GaSb quantum wells should be a topologically non-trivial QSH phase protected by the bulk gap.

This seemingly simple conclusion is complicated by the unique features of type II quantum wells: the electron-subband and hole-subband are separated in two different layers. There are several separate consequences of this

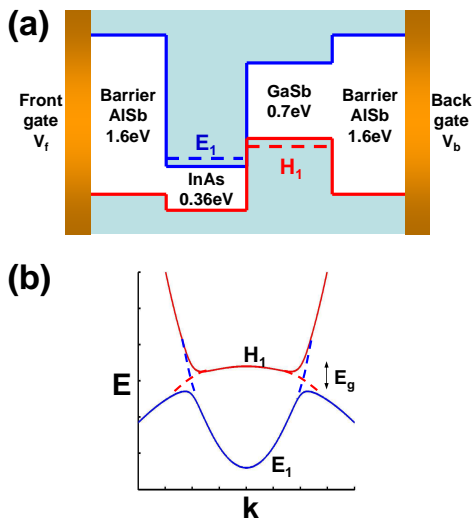


FIG. 1: (a) Band gap and band offset diagram for asymmetric AlSb/InAs/GaSb quantum wells. The left AlSb barrier layer is connected to a front gate while the right barrier is connected to a back gate. The  $E_1$  subband is localized in the InAs layer and  $H_1$  is localized in the GaSb layer. Outer AlSb barriers provide an overall confining potential for electron and hole states. (b) Schematic band structure diagram. The dashed line shows the crossing of the  $E_1$  and  $H_1$  states in the inverted regime, and due to the hybridization between  $E_1$  and  $H_1$ , the gap  $E_g$  appears.

fact. First, the hybridization between  $E_1$  and  $H_1$  is reduced, but this is just a quantitative correction. Second, since there is no inversion symmetry in the quantum well growth direction, SIA terms may be large enough to compete with the reduced hybridization. In addition, BIA may also play a role for this system. Therefore, both SIA and BIA must be included properly to make a correct prediction, while in HgTe/CdTe quantum wells these two types of terms were ignored because BIA terms are small when compared with the hybridization, and the quantum well was symmetric which minimizes SIA. Finally, since the electron and hole subbands lie in two different layers, there is an automatic charge transfer between the layers which yields a coexistence of p-type and n-type carriers. Consequently, a self-consistent treatment of Coulomb energy is necessary to account for this effect. In the following, we will discuss all of these issues and conclude that the QSH phase exists in an experimentally viable parameter range.

The materials in these quantum wells have the zinc-blende lattice structure and direct gaps near the  $\Gamma$  point and are thus well-described by the 8-band Kane model[15]. We will construct an effective 4-band model using the same envelope function approximation procedure as the Bernevig-Hughes-Zhang (BHZ) model[1]; albeit a more complex one due to the SIA and BIA terms. The Hamiltonian naturally separates into three distinct

parts

$$\mathcal{H} = H_0 + H_{BIA} + H_{SIA}. \quad (1)$$

In the basis  $\{|E_1+\rangle, |H_1+\rangle, |E_1-\rangle, |H_1-\rangle\}$ , and keeping terms only up to quadratic powers of  $\mathbf{k}$ , we have

$$H_0 = \epsilon(k)\mathbf{I}_{4\times 4} + \begin{pmatrix} \mathcal{M}(k) & Ak_+ & 0 & 0 \\ Ak_- & -\mathcal{M}(k) & 0 & 0 \\ 0 & 0 & \mathcal{M}(k) & -Ak_- \\ 0 & 0 & -Ak_+ & -\mathcal{M}(k) \end{pmatrix} \quad (2)$$

where  $\mathbf{I}_{4\times 4}$  is the  $4 \times 4$  identity matrix,  $\mathcal{M}(k) = M_0 + M_2k^2$  and  $\epsilon(k) = C_0 + C_2k^2$ . This is simply the Hamiltonian used by BHZ. The zinc-blende structure has two different atoms in each unit cell, which breaks the bulk inversion symmetry and leads to additional terms in the bulk Hamiltonian[16]. When projected onto the lowest subbands the BIA terms are

$$H_{BIA} = \begin{pmatrix} 0 & 0 & \Delta_e k_+ & -\Delta_0 \\ 0 & 0 & \Delta_0 & \Delta_h k_- \\ \Delta_e k_- & \Delta_0 & 0 & 0 \\ -\Delta_0 & \Delta_h k_+ & 0 & 0 \end{pmatrix}. \quad (3)$$

Finally the SIA term reads

$$H_{SIA} = \begin{pmatrix} 0 & 0 & i\xi_e k_- & 0 \\ 0 & 0 & 0 & 0 \\ -i\xi_e^* k_+ & 0 & 0 & 0 \\ 0 & 0 & 0 & 0 \end{pmatrix}. \quad (4)$$

Here we recognize the SIA term as the electron  $k$ -linear Rashba term; the heavy-hole  $k$ -cubic Rashba term is neglected. The parameters  $\Delta_h, \Delta_e, \Delta_0, \xi_e$  depend on the quantum well geometry.

Now we address, from pure band structure considerations, whether or not a QSH phase exists in this model. Without  $H_{BIA}$  and  $H_{SIA}$  the Hamiltonian is block diagonal and each block is exactly a massive Dirac Hamiltonian in  $(2+1)d$ . By itself, each block breaks time-reversal symmetry, but the two  $2 \times 2$  blocks are time-reversal partners so that the combined system remains time-reversal invariant. As mentioned, this is the pure BHZ model and from their argument we know that there is a topological phase transition signalled by the gap closing condition  $M_0 = 0$ , and the system is in QSH phase when  $M_0/M_2 < 0$ . When  $H_{BIA}$  and  $H_{SIA}$  terms are included, the two blocks of  $H_0$  are coupled together and the analysis in BHZ model does not directly apply. However, the QSH phase is a topological phase of matter protected by the band gap[3, 4, 5]. In other words, if we start from the Hamiltonian  $H_0$  in the QSH phase and turn on  $H_{BIA}$  and  $H_{SIA}$  adiabatically, the system will remain in the QSH phase as long as the energy gap between  $E_1$  and  $H_1$  remains finite. With realistic parameters for an InAs/GaSb/AlSb quantum well obtained from the 8-band Kane model, the adiabatic connection between the inversion-symmetric Hamiltonian  $H_0$  and the full Hamiltonian  $\mathcal{H}$  was verified for the proper parameter regime,

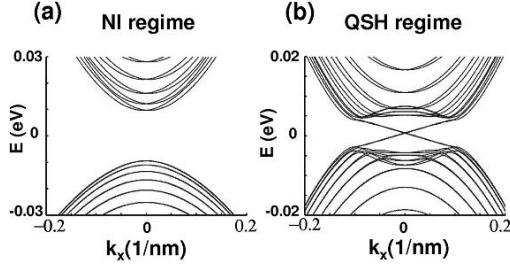


FIG. 2: The energy dispersions of Hamiltonian (1) on a cylindrical geometry with open boundary conditions along the  $y$ -direction and periodic boundary conditions along the  $x$ -direction. (a) The dispersion for the quantum well with GaSb layer thickness  $d_1 = 10\text{nm}$  and InAs layer thickness  $d_2 = 8.1\text{nm}$ , which is a normal insulator with no edge states. (b) The dispersion for  $d_1 = d_2 = 10\text{nm}$  quantum well which is a QSH insulator with one pair of edge states. A tight-binding regularization with lattice constant  $a = 20\text{\AA}$  is used in this calculation.

which supports the existence of a QSH phase in this system. Though the BIA and SIA terms do not destroy the QSH phase, they do modify the quantum phase transition between the QSH phase and normal insulator (NI). The transition (gap-closing) will generically occur at finite- $\mathbf{k}$  rather than at the  $\Gamma$  point, and a nodal region between QSH and NI phases can possibly appear in the phase diagram[17, 18, 19, 20].

A more direct way of identifying the QSH phase is to study the edge state spectrum. There are always an odd number of Kramer's pairs of edge states confined on the boundary of a QSH insulator, and an even number pairs (possibly zero) for the boundary of the NI phase. The edge state energy spectrum of the effective model (1) can be obtained by solving this model with a simple tight-binding regularization in a cylindrical geometry, the result of which is shown in Fig. 2. We find one Kramer's pair of edge states with opposite spin on each edge for the QSH side, and no edge states for the NI side. This again confirms the existence of QSH phase in this model.

To study the InAs/GaSb/AlSb quantum well system more systematically and quantitatively, we confirm the above analysis by numerically solving the realistic 8-band Kane model. In the inverted regime, there exists an intrinsic charge transfer between the InAs layer and GaSb layer. Therefore, we need to take into account the built-in electric field. The energy dispersions for different well thicknesses are shown in Fig. 3 (a)-(c), where we fix the GaSb layer thickness  $d_1 = 10\text{nm}$  and vary the thickness of InAs layer  $d_2$ . The system is gapped for a generic value of  $d_2$ . However, at a critical thickness  $d_{2c} = 9\text{nm}$  (Fig 3 (b)) a crossing at finite  $\mathbf{k}$  occurs between the subbands  $E_1$  and  $H_1$ , which marks the phase transition point between the QSH and NI phases. According to the above adiabatic continuity argument, we know that the quantum well is in a NI state for  $d_2 < d_{2c}$  (Fig. 3 (a)) and

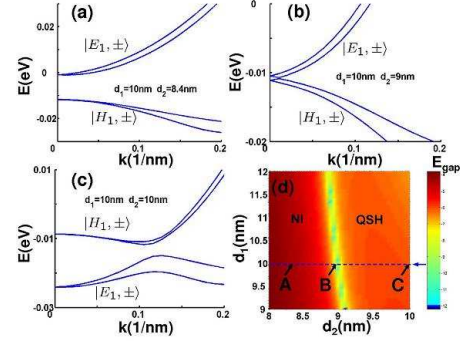


FIG. 3: (a)-(c) The energy dispersions calculated from the 8-band Kane model for three well configurations, where  $d_1$  and  $d_2$  are the thickness of GaSb layer and InAs layer, respectively. (d) The energy gap variation in  $d_1 - d_2$  plane, where brighter colors represent a smaller gap. A, B and C on the dashed blue line indicate respectively the place where (a), (b) and (c) are plotted. NI and QSH denote the phases in the corresponding region of parameter space.

QSH state for  $d_2 > d_{2c}$  (Fig. 3 (c)). As the band inversion is only determined by the relative positions of  $E_1$  and  $H_1$ , the quantum wells with other values of  $d_1$  behave essentially the same. As the QSH phase and NI phase are always separated by a gap closing point, we can determine the  $d_1 - d_2$  phase diagram via the energy gap. As shown in Fig. 3 (d), two gapped regimes (in red) are separated by a critical line (brightly colored) in the  $d_1, d_2$  plane. The quantum well configurations shown in Figs. 3 (a), (b) and (c) are indicated by points A, B and C, respectively. Due to the adiabatic continuity, an entire connected gapped region in the phase diagram is in the NI (QSH) phase once one point in it is confirmed to be in this phase. Since Fig. 3 (a) corresponds to the NI phase and (c) the QSH phase, we identify the right side of the diagram as the QSH regime and the left side as the NI regime.

One advantage of the InAs/GaSb/AlSb quantum wells is that due to the large built-in electric field, the QSH-NI phase transition can be easily tuned by external gate voltages. When we tune the gate voltage, both the band structure and the Fermi level are adjusted simultaneously. Since the QSH effect can only occur when the Fermi level lies in the gap, we need two gates in order to independently tune the relative position between the  $E_1$  and  $H_1$  band edges and the Fermi level. In fact, such a dual-gate geometry has already been realized experimentally in InAs/GaSb/AlSb quantum wells[10]. In the present work, we performed a self-consistent Poisson-Schrodinger type calculation[12, 13, 14] for such a dual-gate geometry shown in Fig. 1 (a). To simplify the calculation, we take the thickness of the AlSb barrier layers to be much smaller than that in realistic experiments, which has a negligible effect in the quantum well except for a rescaling of  $V_f$  and  $V_b$ . We also neglect the weak ef-

fects of subband anisotropy and intrinsic donor defects at the InAs/GaSb interface. None of these simplifications should affect our results qualitatively.

For fixed  $d_1 = d_2 = 10$  nm we explored the  $V_f - V_b$  phase diagram as shown in Fig. 4. There are six distinct regions in the figure. The dotted black line shows the gap closing transition between the inverted and non-inverted regimes. In parameter regions I,II,III the system has an inverted band structure, but only region II is in the QSH phase with the Fermi level tuned inside the bulk gap. Region I (III) is described by the same Hamiltonian as the QSH phase, but with finite hole (electron) doping. In the same way, region V is the NI phase and IV, VI are the corresponding p-doped and n-doped normal semiconductors. Thus, by tuning  $V_f$  and  $V_b$  to the correct range, one can easily get the phase transition between QSH phase II and NI phase V.

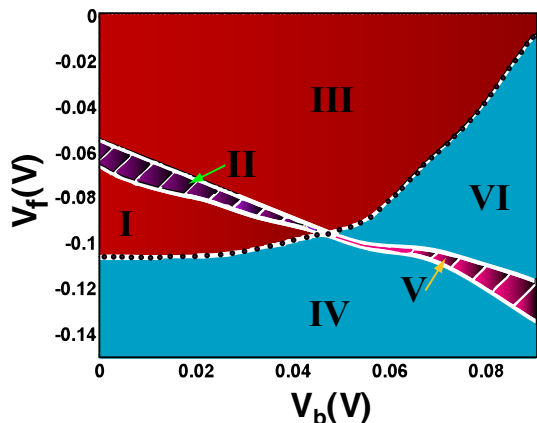


FIG. 4: The phase diagram for different front ( $V_f$ ) and back ( $V_b$ ) gate voltages. Regions I,II,III are in the inverted regime, in which the striped region II is the QSH phase with Fermi-level in the bulk gap, and I, III are the p-doped and n-doped inverted system. Regions IV,V,VI are in the normal regime, in which the striped region V is the NI phase with Fermi level in the bulk gap, and IV, VI are the p-doped and n-doped normal semiconductors. The well configuration is set as  $d_1 = d_2 = 10$  nm, and the AlSb barrier thickness is taken 30nm on each side in the self-consistent calculation.  $V_f$  and  $V_b$  are defined with respect to the Fermi level in the quantum well.

Compared to the similar proposal of a gate-induced phase transition in asymmetric HgTe/CdTe quantum wells[21], the InAs/GaSb/AlSb quantum well is much more sensitive to the gate voltage, which makes it much easier to realize such a transition experimentally. Physically, this comes from the fact that the electron and hole wavefunctions are centered in separate layers, so that the effect of the gate voltage on them is highly asymmetric. This simple mechanism allows us to investigate the quantum phase transition from the NI to the QSH state in-situ, through the continuous variation of the gate voltage, rather than the discrete variation of the quantum well thickness. It is also useful for developing a QSH FET. The FET is in an ‘OFF’ state when the Fermi level lies inside the normal insulating gap. Then, by adjusting the gate voltages the FET can be flipped to the ‘ON’ state by passing through the transition to the QSH phase, where the current is carried only by the dissipationless edge states. This simple device can be operated with reasonable voltages as seen in Fig. 4 but would be more promising if one could enlarge the bulk insulating gap to support room temperature operation.

In conclusion, we propose that the QSH state can be realized in InAs/GaSb quantum wells. We presented both simple arguments based on effective model and realistic self-consistent calculations. In addition we have proposed an experimental setup to electrically control the quantum phase transition from the normal insulator to the QSH phase. This principle could be used to construct a QSH FET device with minimal dissipation.

We would like to thank B. F. Zhu for the useful discussion. This work is supported by the NSF under grant numbers DMR-0342832, the US Department of Energy, Office of Basic Energy Sciences under contract DE-AC03-76SF00515 and by the Focus Center Research Program (FCRP) Center on Functional Engineered Nanoarchitectonics (FENA). CXL acknowledges the support of China Scholarship Council, the NSF of China (Grant No.10774086, 10574076), and the Program of Basic Research Development of China (Grant No. 2006CB921500).

[1] B. A. Bernevig, T. L. Hughes, and S.C. Zhang, *Science* **314**, 1757 (2006).  
 [2] M. Konig, S. Wiedmann, C. Brune, A. Roth, H. Buhmann, L. W. Molenkamp, X.-L. Qi, and S.-C. Zhang, *Science* **318**, 766 (2007).  
 [3] C. L. Kane and E. J. Mele, *Phys. Rev. Lett.* **95**, 226801 (2005).  
 [4] C. J. Wu, B. A. Bernevig, and S. C. Zhang, *Phys. Rev. Lett.* **96**, 106401 (2006).  
 [5] C. Xu and J. Moore, *Phys. Rev. B* **73**, 045322 (2006).

[6] L. L. Chang and L. Esaki, *Surf. Sci.* **98**, 70 (1980).  
 [7] M. Altarelli, *Phys. Rev. B* **28**, 842 (1983).  
 [8] M. J. Yang, C. H. Yang, B. R. Bennett, and B. V. Shanabrook, *Phys. Rev. Lett.* **78**, 4613 (1997).  
 [9] M. Lakrimi, S. Khym, R. J. Nicholas, D. M. Symons, F. M. Peeters, N. J. Mason, and P. J. Walker, *Phys. Rev. Lett.* **79**, 3034 (1997).  
 [10] L. J. Cooper, N. K. Patel, V. Drouot, E. H. Linfield, D. A. Ritchie, and M. Pepper, *Phys. Rev. B* **57**, 11915 (1998).

- [11] E. Halvorsen, Y. Galperin, and K. A. Chao, Phys. Rev. B **61**, 16743 (2000).
- [12] I. Lapushkin, A. Zakharova, S. T. Yen, and K. A. Chao, J. Phys: Condens. Matter **16**, 4677 (2004).
- [13] I. Semenikhin, A. Zakharova, K. Nilsson, and K. A. Chao, Phys. Rev. B **76**, 035335 (2007).
- [14] Y. Naveh and B. Laikhtman, Phys. Rev. Lett. **77**, 900 (1996).
- [15] E.O. Kane, J. Phys. Chem. Solids **1**, 249 (1957).
- [16] R. Winkler, *Spin-Orbit Coupling Effects in Two-Dimensional Electron and Hole Systems* (Springer Tracts in Modern Physics, 2003).
- [17] S. Murakami, S. Iso, Y. Avishai, M. Onoda, and N. Nagaosa, Physical Review B **76**, 205304 (2007).
- [18] X. Dai, T. L. Hughes, X.-L. Qi, Z. Fang, and S.-C. Zhang, arXiv:0705.1516, to be published on Phys. Rev. B.
- [19] M. Koenig, H. Buhmann, L. W. Molenkamp, T. L. Hughes, C.-X. Liu, X.-L. Qi, and S.-C. Zhang, arXiv:0801.0901 (2008).
- [20] T. L. Hughes, C.-X. Liu, X.-L. Qi, and S.-C. Zhang, in preparation.
- [21] W. Yang, K. Chang, and S. C. Zhang, arXiv:0711.1900.